Sorting of Cells Using Flow Channel with Oblique Micro Grooves

Yusuke TAKAHASHI, Shigehiro HASHIMOTO, Yoshinori HORI, Takuya TAMURA

Biomedical Engineering, Department of Mechanical Engineering,
Kogakuin University, Tokyo, 163-8677, Japan
http://www.mech.kogakuin.ac.jp/labs/bio/

ABSTRACT

Micro grooves have been designed to sort biological cells, which flows through a micro channel *in vitro*. The micro groove of the rectangular shape (0.0045 mm depth, and 0.2 mm length) has been fabricated on the surface of the polydimethylsiloxane (PDMS) disk by the photolithography technique. Variation has been made on the width (0.03 mm < w < 0.05 mm) and on the angle between the longitudinal direction of the groove and the flow direction (45 degrees, 90 degrees) of the groove. A rectangular flow channel (0.05 mm height × 2 mm width × 15 mm length) has been constructed between two transparent PDMS disks. Four kinds of cells were used in the test: C2C12 (mouse myoblast cell line), MC3T3-E1 (mouse osteoblast precursor cell), Hepa1-6 (mouse hepatoma cell), and Neuro-2a (mouse neural crest-derived cell). A flow velocity of the suspension of cells was controlled by the pressure difference between the inlet and the outlet. Neuro-2a often moves to the counter direction against the flow in the groove. The shift movement along the oblique groove depends on the several parameters: the diameter of cells, the width of the groove, the velocity of the cell, and the kinds of cells.

Keywords: Biomedical Engineering, MC3T3E1, Hepa1-6, C2C12, Neuro-2a, Micro Groove and Polydimethylsiloxane.

1. INTRODUCTION

A flowing cell is captured to a wall of a flow path. Several cells adhere to the internal wall of the blood vessel, when the part of the wall has a defect. The morphology of the defect might govern the capture of cells. The capture also might depend on the property of the cell. The cancer cell transits from the original place to another place, and proliferates to make a tumor at another place. The transition occurs through the blood vessels and the lymph vessels. The cancer cells adhere to the inner wall of the vessels.

The effect of the surface property of the scaffold on the cell has been studied in the previous studies [1-8]. Several micro-fabrication processes have been designed to control adhesion of biological cells *in vitro*, and to simulate the morphology of the microcirculation [9, 10]. The photolithography technique enables manufacturing the micro-morphology. The micro-fabrication technique has also been applied to design microfluidic systems *in vitro* [11-19].

Cells roll over on the surface of the wall in the shear flow, and make adhesion to the wall. The surface was modified to capture flowing cells [11-13, 19]. The technique will also be applied to handle cells in diagnostics *in vitro*.

In the present study, the movement of the single cell flowing at the micro groove, which is manufactured by the photolithography technique, has been analyzed *in vitro*.

2. METHODS

Micro Grooves
For trapping cells, several micro grooves of the rectangular shape (0.0045 mm depth, and 0.2 mm length) have been fabricated on the surface of the polydimethylsiloxane (PDMS) plate with the photolithography technique. Several grooves are arranged on the same wall. At the groove arrangement from upstream to downstream, variation has been made on the width of the groove: 0.03 mm, 0.04 mm, and 0.05 mm (Fig. 1). Variation has also been made on the angle between the longitudinal direction of the groove and the flow direction: 45 degrees, and 90 degrees (Fig. 2).

Photomask
The slide glass (Matsunami) plate (38 mm length, 26 mm width, and 1.0 mm thickness) was used for the base of the photomask (Fig. 3). Before the deposition of titanium, the surface of the glass plate was cleaned by the oxygen (30 cm^3/min, 0.1 Pa) plasma ashing for five minutes at 100 W by the reactive ion etching system (FA-1, Samco International, Kyoto, Japan). Titanium was deposited on the surface of the glass plate with 200 nm thickness in the spattering system (back pressure < 9×10^{-4} Pa, RF100W, 0.5 Pa, 8 min, L-210S-FH Canon Anelva Corporation, Kawasaki, Japan).
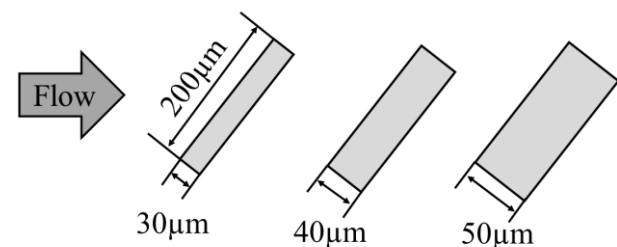
Fig. 1: Dimension of three types of oblique grooves.

To improve affinity to photoresist material, HMDS (hexamethyldisilazane: Tokyo Chemical Industry Co., Ltd., Tokyo) was coated on the glass plate at 3000 rpm for 30 s with the spin coater (1H-DX2, Mikasa Co. Ltd., Tokyo). The positive photoresist material of OFPR-800LB (Tokyo Ohka Kogyo Co., Ltd, Tokyo, Japan) was coated on the titanium with the spin coater (at 7000 rpm for 30 s). The photoresist was baked in the oven (DX401, Yamato Scientific Co., Ltd) at 368 K for five minutes.

The pattern for the groove was drawn on the mask with a laser drawing system (DDB-201K-KH, Neoark Corporation, Hachioji, Japan). To control the dimension of the pattern on the mold with the laser drawing system, the parameters were selected as follows: the voltage of 3.26 V, the velocity of 0.137 mm/s, the acceleration of 0.5 mm/s^2, and the focus offset at +3.17.

The photoresist was baked in the oven (DX401) at 368 K for five minutes. The photoresist was developed with tetra-methyl-ammonium hydroxide (NMD-3, Tokyo Ohka Kogyo Co., Ltd., Kawasaki, Japan) for five minutes, rinsed with the distilled water (300 rpm, 30 s), and dried by the spin-dryer (1100 rpm, 30 s, with N$_2$ gas, SF-250, Japan Create Co., Ltd., Tokorozawa, Japan).

The titanium coated plate was etched with the plasma gas using RIE-10NR (Samco International, Kyoto, Japan). For etching, the gas of SF$_6$ (50 cm^3/min at 1013 hPa) with Ar (50 cm^3/min at 1013 hPa) was applied at 100 W at 4 Pa for six minutes. The residual OFPR-800LB was removed by acetone dipped for one minute. The plate was dipped in the distilled water in one minute, after it is dipped in ethanol for one minute. The plate was dried by the spin-dryer: 300 rpm for 30 s with the distilled water, and 1100 rpm for 30 s with N$_2$ gas.

Lower Plate
The slide glass (Matsunami) plate (38 mm length, 26 mm width, and 1.0 mm thickness) was used for the base of the mold (Fig. 4). The surface of the glass plate was hydrophilized by the oxygen (30 cm^3/min, 0.1 Pa) plasma ashing for five minutes at 100 W by the reactive ion etching system (FA-1).

The epoxy based negative photo-resist material (SU8-5: Micro Chem Corp., MA, USA) was coated on the glass at 2500 rpm for 30 s with a spin coater. The photoresist was baked in the oven (DX401) at 368 K for five minutes.
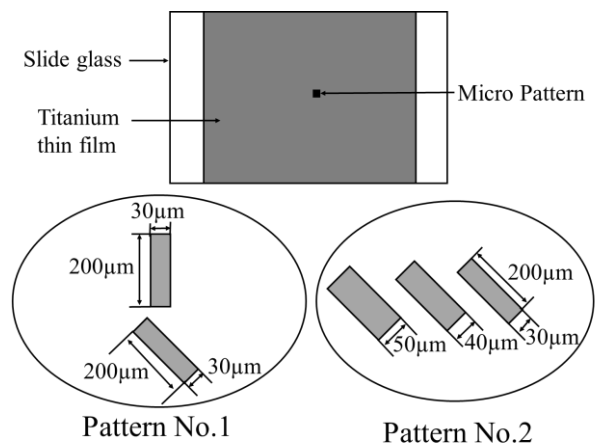

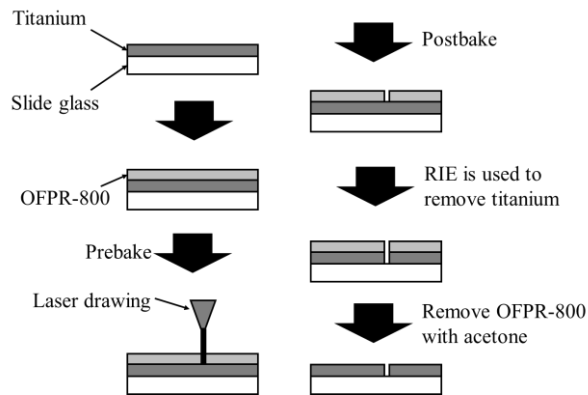**Fig. 2:** Two patterns of microgrooves on photomask.

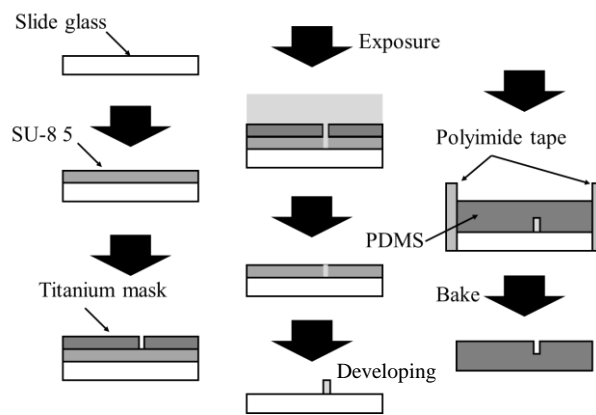**Fig. 3:** Photolithography process for photomask.

Fig. 4: Photolithography process for lower plate.

The photoresist was exposed to the UV light through the photomask in the mask aligner (M-1S, Mikasa Co. Ltd., Japan) at 15 mW/cm^2 for 25 s. The photoresist was baked in the oven at 393 K for seven minutes. The photo-resist was developed with SU8 developer (Nippon Kayaku Co., Ltd, Tokyo, Japan) for five minutes to make micro rectangular ridges, where the laser beam was radiated.

The glass surface with the micro pattern was rinsed with IPA (2-propanol, Wako Pure Chemical Industries, Ltd.) for one minute. The plate was dried by the spin-dryer: 300 rpm for 30 s with the distilled water, and 1100 rpm for 30 s with N$_2$ gas.

After the plate was enclosed with a peripheral wall of polyimide tape, PDMS (Sylgard 184 Silicone Elastomer Base, Dow Corning Corp., MI, USA) was poured with the curing agent (Sylgard 184 Silicone Elastomer Curing Agent, Dow Corning Corp., MI, USA) on the plate. The volume ratio of PDMS to curing agent is ten to one. After degassing, PDMS was baked at 368 K for twenty minutes in the oven.

Upper Plate
The slide glass (Matsunami) plate (38 mm length, 26 mm width, and 1.0 mm thickness) was used for the base of the mold (Fig. 5). The polyimide tape (0.055 mm thickness, 10 mm width) was pasted at the center of the glass plate. The tape was cut (mm × mm) by the ultra-short pulse laser (IFRIT, Cyber Laser Inc., Tokyo, Japan) to make the mold for the upper part of the flow channel.

After the glass plate was enclosed with a peripheral wall of polyimide, PDMS was poured with the curing agent on the plate (Fig. 6). The volume ratio of PDMS to curing agent is ten to one. After degassing, PDMS was baked at 368 K for twenty minutes in the oven (DX401). Two holes (diameter of 5 mm) with the interval of 5 mm were punched by a punching tool to make the inlet and the outlet (Fig. 7a).

Flow System
Both the upper and the lower plates were exposed to the oxygen gas (0.1 Pa, 30 cm^3/min) in the reactive ion etching system (FA-1) (oxygen plasma ashing, 50 W, for thirty seconds). Immediately after ashing, the upper disk adheres (plasma bonding) to the lower disk to make the flow path (15 mm length × 2 mm width × 0.055 mm height) between them. The flow channel is placed on the stage of the inverted phase-contrast microscope (IX71, Olympus Co., Ltd., Tokyo) (Fig. 7b).

Flow Test
Four kinds of cells were used in the test: C2C12 (passage < 10, mouse myoblast cell line originated with cross-striated muscle of C3H mouse), MC3T3-E1 (passage nine, osteoblast precursor cell line derived from mouse calvaria), Hepa1-6 (passage six, mouse hepatoma cell line of C57L mouse), and Neuro-2a (passage seven, mouse neural crest-derived cell line)

Cells were cultured with the D-MEM (Dulbecco's Modified Eagle's Medium) containing 10% FBS and 1% of Antibiotic-Antimycotic (penicillin, streptomycin and amphotericin B, Life Technologies) in the incubator for one week.

The inner surface of the flow channel was hydrophilized by the oxygen (30 cm^3/min, 0.1 Pa) plasma ashing for one minute at 100 W by the reactive ion etching system (FA-1), and prefilled with the bovine serum albumin solution for thirty minutes at 310 K.

Before the flow test, the cells were exfoliated from the plate of the culture dish with trypsin, and suspended in the D-MEM (Dulbecco's Modified Eagle's Medium). The suspension of cells (20000 cells/cm^3, 0.06 cm^3) was poured at the inlet of the flow channel. The flow occurs by the pressure difference between the inlet and the outlet. The inlet hole (the depth of 3 mm and the diameter of 5 mm) makes the pressure head.
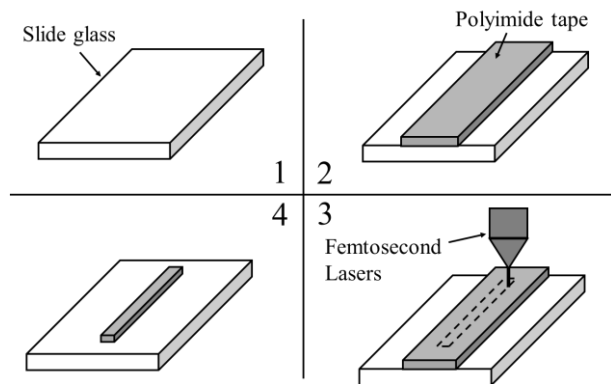

Fig. 5: Mold for upper plate.
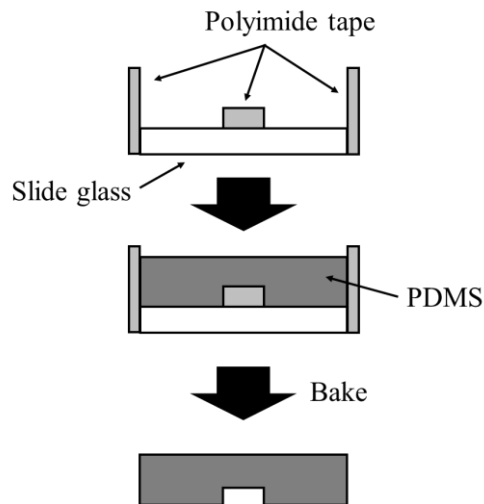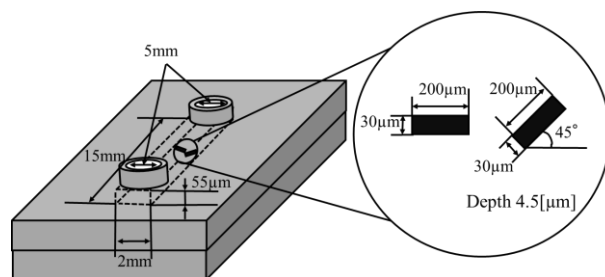
Fig. 6: Upper plate.

**Fig. 7a:** Flow channel.
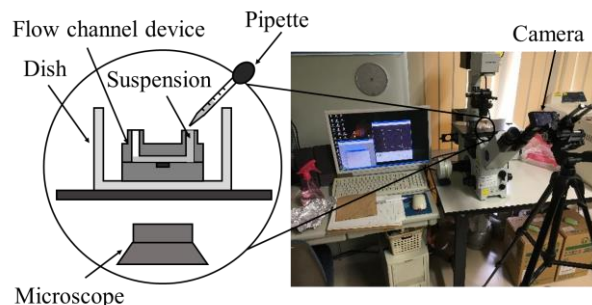
Fig. 7b: Experimental system.

Each cell rolling over the micro grooves was observed by the microscope, and recorded by the camera (DSC-RX100M4, Sony Corporation, Japan), which is set at the eyepiece of the microscope. The movement of each cell was analyzed by "Kinovea" at the video images: 30 frames per second. At the images, the contour of each cell was traced with "Image J", and approximated to the circle to calculate the diameter (D) (Fig. 8).

The velocity of each cell around the groove was traced on the component parallel to the direction of the main flow of the velocity of the cell: immediately before the groove (v_0) and in the groove (v_1) (Fig. 9). The travel distance of each cell along the groove was traced on the component (x) perpendicular to the main flow direction.

[Projected area]

Fig. 8: Evaluation of dimension of cell (white circle) at optical microscope image (right).

[Velocity]   [Vertical travel distance]
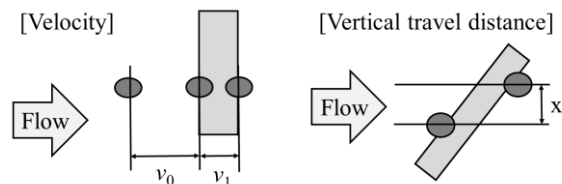
Fig. 9: Evaluation of movement of cell at groove: velocity before groove (v_0), in groove (v_1): vertical travel distance (x).
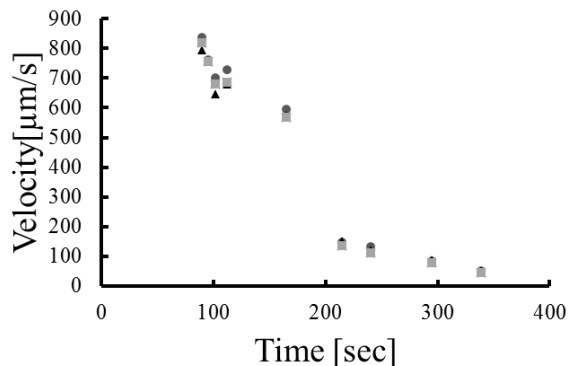

Fig. 10a: MC3T3-E1 (red circle) before groove (left), in groove (right); flow from left to right: optical microscope image.

0.1 mm
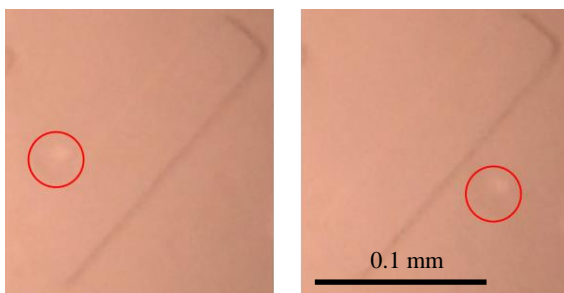
Fig. 10b: Neuro2a (red circle) before groove (left), after groove (right); flow from left to right: optical microscope image.
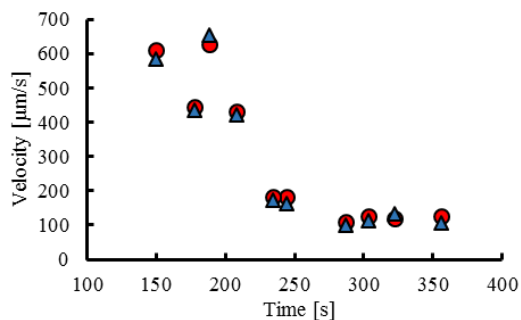
Fig. 11: Velocity of C2C12 vs. time: before groove (circle), and in groove (triangle): 90 degrees groove.

Fig. 12: Velocity of C2C12 in three width type of oblique (45 degrees) groove vs. time: 0.03 mm (circle), 0.04 mm (square), and 0.05 mm (triangle).

3. RESULTS

Fig. 10 exemplifies the cell approaching to the groove (left) and departing from the groove (right): MC3T3-E1 (a), and Neuro2a (b). The direction of the flow is from left to right in Fig. 10. Most of cells travel along the groove to the downstream to show positive x (Fig. 10a). Many cells of Neuro2a migrate in the groove to the upstream to show negative x (Fig. 10b).

Fig. 11 shows the velocity of C2C12 around the groove of 90 degrees: before the groove (v_0) and in the groove (v_1). Each pair of data shows v_0 and v_1 of the same cell. The velocity decreases with the time, because the pressure head at the inlet decreases with time. The velocity in the groove is slower than that before the groove, except at the velocity of 0.62 mm/s.

Fig. 12 shows the velocity (v_1) of C2C12 in the groove of 45 degrees. Each group of three data shows v_1 of the same cell at each width of the groove, respectively. The velocity decreases with the time, because the pressure head at the inlet decreases with time. The velocity in the groove tends to be slower in the wider groove at the higher velocity.

Figs. 13, 14 and 15 show the shifted distance (x) along the groove, which is the component perpendicular to the main flow direction, in relation to the diameter (D) of each cell: C2C12 (Fig. 13), MC3T3-E1 (Fig. 14), and Hepa1-6 (Fig. 15), respectively. Each marker shows the variation of the width of the groove: 0.03 mm, 0.04 mm, and 0.05 mm, respectively. Each dotted line shows the approximated linear relationship at the corresponding data. The distance (x) tends to increase with decrease of the diameter of the cell of C2C12 (Fig. 13), and of MC3T3-E1 (Fig. 14). The tendency is remarkable at the groove of the narrower width (0.03 mm). In Hepa1-6, on the other hand, the distance (x) varies with no significant relation to the diameter (D) of each cell.

Fig. 16 show the shifted distance (x) along the groove in relation to the velocity immediately before the groove (v_0) of Hepa1-6. Each marker shows the variation of the width of the groove: 0.03 mm, 0.04 mm, and 0.05 mm, respectively. Each dotted line shows the approximated linear relationship at the corresponding data. The distance (x) tends to increase with decrease of the velocity immediately before the groove (v_0).
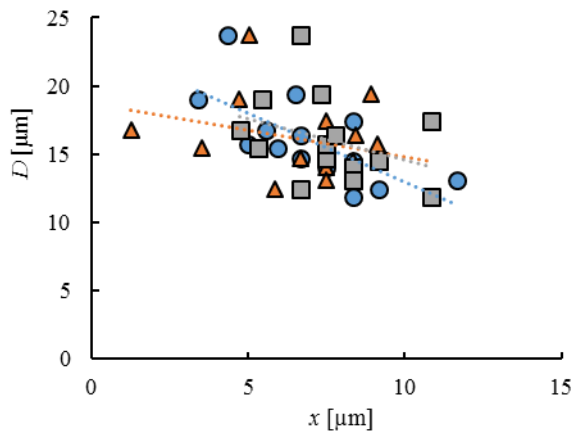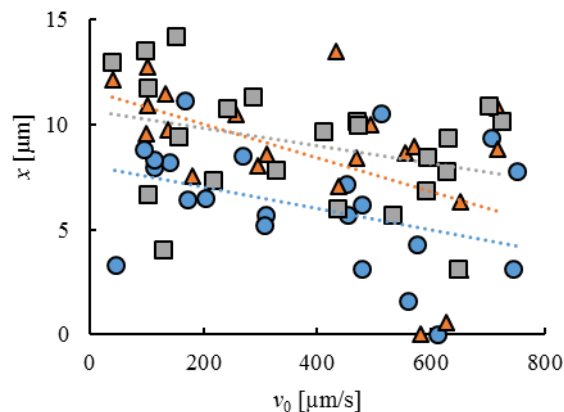
Fig. 13: Diameter (*D*) of C2C12 in relation to shifted distance along groove (*x*): circle, 0.03 mm; triangle, 0.04 mm; square, 0.05 mm width: dotted line, approximated line.
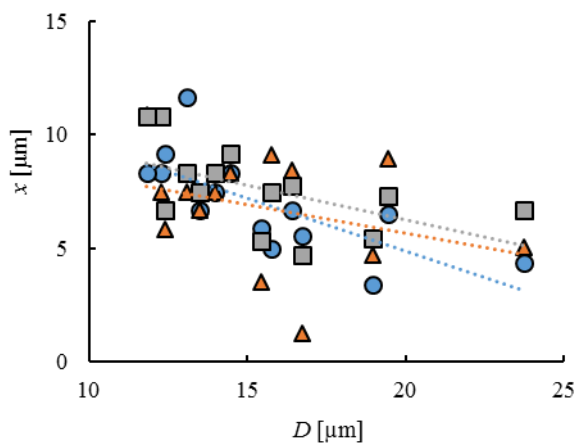
Fig. 14: Diameter (*D*) of MC3T3-E1 in relation to shifted distance along groove (*x*): circle, 0.03 mm; triangle, 0.04 mm; square, 0.05 mm width: dotted line, approximated line.
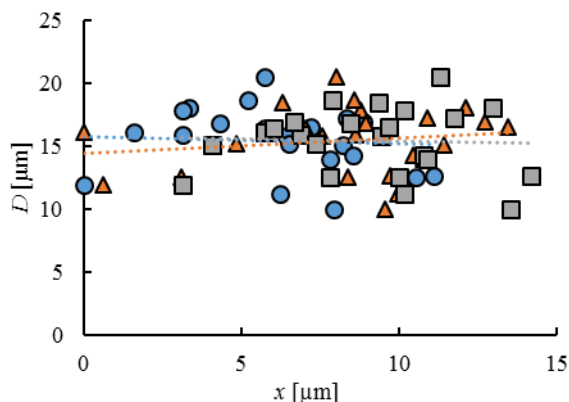
Fig. 15: Diameter (*D*) of Hepa1-6 in relation to shifted distance along groove (*x*): circle, 0.03 mm; triangle, 0.04 mm; square, 0.05 mm width: dotted line, approximated line.

Fig. 16: Velocity (v_0) of Hepa1-6 in relation to shifted distance along groove (*x*): circle, 0.03 mm; triangle, 0.04 mm; square, 0.05 mm width: dotted line, approximated line.

4. DISCUSSION

The rectangular grooves has been successfully manufactured on the wall of the micro fluid channel. The dimension of the grooves were confirmed by the laser microscope [13]. Several kinds of systems were designed for the cell culture in flow [11-21] and for the cell sorting *in vitro* [22-25]. The micromachining technique has been applied to cell technology. The microfluidic system was applied to sort biological cells, and to trap biological cells [11-13]. The experimental results might contribute to analyze adhesive mechanism of cancer cell during metastasis. The micro trap might simulate adhesive mechanism of flowing cells. Neuro-2a, for example, might be highly adhesive.

Several fluid flow system were used in the previous studies. In the previous studies, cylindrical [11] and half cylindrical [12] holes were used for the trap of cells. The asymmetrical hole might be suitable for trap than the symmetrical hole. The depths of the micro holes were between 0.002 mm and 0.01 mm in the previous studies [11-13]. In the present study, the depth of the grooves is 0.0045 mm, which is smaller than the diameter of the cells. The deeper hole may have advantage to trap cells. At the shallower trap, on the other hand, it is not easy to tarp a cell. The trap of the appropriate dimension may distinguish cells. The duration of the trapped time of the cell might relate to interaction between the micro hole and the cell: affinity between the cell and the surface of the micro pattern, or deformability of the cell.

The results of the present study show that the movement of cell travelling on the wall is modified by the oblique micro groove on the wall under the cell velocity lower than 1 mm/s. The angle of 45 degrees between the longitudinal direction of the groove and the flow direction is effective to shift the streamline of the cell. The shift movement along the oblique groove depends on the several parameters: the diameter of cells, the width of the groove, the velocity of the cell, and the kinds of cells. As the diameter of the cell decreases, the traveling length along the groove increases. The movement might be related not only to the diameter but also to the deformability of the cell. The cell density in the suspension is very low in this study to reduce the interaction between the cells. Cells can be sorted by the traveling length along the microgroove.

5. CONCLUSION

Oblique micro grooves have been designed to sort biological cells, which flow through a micro channel *in vitro*. The micro groove of a rectangular shape has been fabricated on the surface of the polydimethylsiloxane plate with the photolithography technique. Four kinds of cells were used in the test: C2C12 (mouse myoblast), MC3T3-E1 (mouse osteoblast), Hepa1-6 (mouse hepatoma cell), and Neuro-2a (mouse neural crest-derived cell). The results show that the cell is trapped by the micro grooves and that the traveling length along the groove is related to the diameter of the cell, to the width of the groove, to the velocity of the cell, and to the kinds of cells.

6. ACKNOWLEDGMENT

REFERENCES

[1] S. Raghavan, R. A. Desai, Y. Kwon, M. Mrksich and C. S. Chen, "Micropatterned Dynamically Adhesive Substrates for Cell Migration", **Langmuir**, Vol. 26, 2010, pp. 17733-17738.

[2] Y. Rondelez, G. Tresset, K.V. Tabata, H. Arata, H. Fujita, S. Takeuchi and H. Noji, "Microfabricated Array of Femtoliter Chambers Allow Single Molecule Enzymology", **Nature Biotechnology**, Vol. 23, No. 3, 2005, pp. 361-365.

[3] H. Miyoshi, J. Ju, S.M. Lee, D.J. Cho, J.S. Ko, Y. Yamagata and T. Adachi, "Control of Highly Migratory Cells by Microstructured Surface Based on Transient Change in Cell Behavior", **Biomaterials**, Vol. 31, No. 33, 2010, pp. 8539-8545.

[4] D. Di Carlo, L.Y. Wu and L.P. Lee, "Dynamic Single Cell Culture Array", **Lab on a Chip**, Vol. 6, 2006, pp. 1445-1449.

[5] H. Liu and Y. Ito, "Cell Attachment and Detachment on Micropattern-Immobilized Poly (N-isopropylacrylamide) with Gelatin", **Lab on a Chip**, Vol. 2, 2002, pp. 175-178.

[6] Y.C. Ou, C.W. Hsu, L.J. Yang, H.C. Han, Y.W. Liu and C.Y. Chen, "Attachment of Tumor Cells to the Micropatterns of Glutaraldehyde (GA)-Crosslinked Gelatin", **Sensors and Materials**, Vol. 20, No. 8, 2008, pp. 435-446.

[7] M.R. King, L.T. Western, K. Rana and J.L. Liesveld, "Biomolecular Surfaces for the Capture and Reprogramming of Circulating Tumor Cells", **Journal of Bionic Engineering**, 2009, Vol. 6, No. 4, pp. 311-317.

[8] H. Hino, S. Hashimoto and F. Sato, "Effect of Micro Ridges on Orientation of Cultured Cell", **Journal of Systemics Cybernetics and Informatics,** Vol. 12, No. 3, 2014, pp. 47-53.

[9] K.A. Barbee, P.F. Davies and R. Lal, "Shear Stress-Induced Reorganization of the Surface Topography of Living Endothelial Cells Imaged by Atomic Force Microscopy", **Circulation Research**, Vol. 74, No. 1, 1994, pp. 163-71.

[10] A. Kamiya, R. Bukhari and T. Togawa, "Adaptive Regulation of Wall Shear Stress Optimizing Vascular Tree Function", **Bulletin of Mathematical Biology**, Vol. 46, No.1, 1984, pp. 127-137.

[11] S. Hashimoto, R. Nomoto, S. Shimegi, F. Sato, T. Yasuda and H. Fujie, "Micro Trap for Flowing Cell", **Proc. 17th World Multi-Conference on Systemics Cybernetics and Informatics**, Vol. 1, 2013, pp. 1-6.

[12] S. Hashimoto, Y. Takahashi, H. Hino, R. Nomoto and T. Yasuda, "Micro Hole for Trapping Flowing Cell", **Proc. 18th World Multi-Conference on Systemics Cybernetics and Informatics**, Vol. 2, 2014, pp. 114-119.

[13] Y. Takahashi, S. Hashimoto, H. Hino, A. Mizoi and N. Noguchi, "Micro Groove for Trapping of Flowing Cell", **Journal of Systemics, Cybernetics and Informatics**, Vol. 13, No. 3, 2015, pp. 1-8.

[14] G. Simone, G. Perozziello, E. Battista, F. De Angelis, P. Candeloro, F. Gentile, N. Malara, A. Manz, E. Carbone, P. Netti and E. Di Fabrizio, "Cell Rolling and Adhesion on Surfaces in Shear Flow. A Model for an Antibody-Based Microfluidic Screening System", **Microelectronic Engineering**, Vol. 98, 2012, pp. 668-671.

[15] J.C. McDonald, D.C. Duffy, J.R. Anderson, D.T. Chiu, H. Wu, O.J.A. Schuller and G.M. Whitesides, "Fabrication of Microfluidic Systems in Poly (dimethylsiloxane)", **Electrophoresis**, Vol. 21, No. 1, 2000, pp. 27-40.

[16] E. Delamarche, A. Bernard, H. Schmid, B. Michel and H. Biebuyck, "Patterned Delivery of Immunoglobulins to Surfaces Using Microfluidic Networks", **Science**, Vol. 276, No. 5313, 1997, pp. 779-781.

[17] K. Funamoto, I.K. Zervantonakis, Y. Liu, C.J. Ochs, C. Kimfg and R.D. Kamm, "A Novel Microfluidic Platform for High-resolution Imaging of a Three-dimensional Cell Culture under a Controlled Hypoxic Environment", **Lab on a Chip**, Vol. 12, 2012, pp. 4855-4863.

[18] L. Liu, K. Loutherback, D. Liao, D. Yeater, G. Lambert, A. Estvez-Torres, J.C. Sturm, R.H. Getzenberg and R.H. Austin, "A Microfluidic Device for Continuous Cancer Cell Culture and Passage with Hydrodynamic Forces", **Lab on a Chip**, Vol. 10, 2010, pp. 1807-1813.

[19] A. Khademhosseini, J. Yeh, S. Jon, G. Eng, K.Y. Suh, J.A. Burdick and R. Langer, "Molded Polyethylene Glycol Microstructures for Capturing Cells within Microfluidic Channels", **Lab on a Chip**, Vol. 4, No. 5, 2004, pp. 425-430.

[20] S. Hashimoto and M. Okada, "Orientation of Cells Cultured in Vortex Flow with Swinging Plate in Vitro", **Journal of Systemics Cybernetics and Informatics**, Vol. 9, No. 3, 2011, pp. 1-7.

[21] S. Hashimoto, F. Sato, H. Hino, H. Fujie, H. Iwata and Y. Sakatani, "Responses of Cells to Flow in Vitro", **Journal of Systemics Cybernetics and Informatics**, Vol. 11, No. 5, 2013, pp. 20-27.

[22] A.Y. Fu, C. Spence, A. Scherer, F.H. Arnold and S.R. Quake, "A Microfabricated Fluorescence-Activated Cell Sorter", **Nature Biotechnology**, Vol. 17, 1999, pp. 1109-1111.

[23] G. Mayer, M.S.L. Ahmed, A. Dolf, E. Endl, P.A. Knolle and M. Famulok, "Fluorescence-activated Cell Sorting for Aptamer SELEX with Cell Mixtures", **Nature Protocols**, Vol. 5, No. 12, 2010, pp. 1993-2004.

[24] M. Brown and C. Wittwer, "Flow Cytometry: Principles and Clinical Applications in Hematology", **Clinical Chemistry**, Vol. 46, No. 8(B), 2000, pp. 1221-1229.

[25] K. Takahashi, A. Hattori, I. Suzuki, T. Ichiki and K. Yasuda, "Non-destructive On-chip Cell Sorting System with Real-time Microscopic Image Processing", **Journal of Nanobiotechnology**, Vol. 2, No. 5, 2004, pp. 1-8.